ISSN 2706-6819 Vol.7, Issue 3: 1-16, DOI: 10.25236/IJFM.2025.070301

Network Pharmacology Prediction and Molecular Docking-Based Strategy for Exploring the Potential Mechanism of the Guanxinjing Capsule in Treating Angina Pectoris

Tao Wen[1,a], Zehui Guo[2,b], Yi Wang[1,c,*]

[1]Tianjin University of Traditional Chinese Medicine, Tianjin, China
[2]Tianjin Academy of Traditional Chinese Medicine Affiliated Hospital, Tianjin, China
[a]1205544580@qq.com, [b]424107569@qq.com, [c]wangyi@tjutcm.edu.cn
**Corresponding author*

Abstract: *The chemical compositions and targets of the Guanxinjing capsule for the treatment of angina pectoris in coronary heart disease were obtained from TCMSP and GeneCards databases. The STRING database and Cytoscape 3.10.1 software were used to construct the PPI network analysis of the intersecting targets to screen out the core targets. The core targets were subjected to GO and KEGG enrichment analyses, and the core components and core targets were subsequently molecularly docked using AutoDock 4 software. AutoDock 4 software was used to perform molecular docking between the core components and core targets to predict the potential mechanism of action for the treatment of AP in CHD. A total of 127 chemical constituents of the Guanxinjing capsule were screened, corresponding to 366 potential targets that intersected with 1613 targets of AP, and 149 intersecting targets were screened. The analysis revealed that the core targets primarily affect the inflammatory response, apoptosis, and involve various signaling pathways, such as the IL-17, TNF, and PI3K-Akt signaling pathways. The analysis of GO function and KEGG pathway enrichment provides valuable insights into the targets' effects. The molecular docking results indicated high affinities between beta-sitosterol, quercetin, stigmasterol, baicalein, kaempferol, luteolin, tanshinone IIA, and salviolone and the core targets TNF, IL6, PPARG, and TP53. The results showed that the Guanxinjing capsule can exert its therapeutic effect on the angina pectoris of CHD through the relevant signaling pathway.*

Keywords: *Guanxinjing Capsule, Angina Pectoris, Coronary Heart Disease, Network Pharmacology, Molecular Docking*

1. Introduction

Coronary heart disease (CHD) is a kind of heart disease induced by underlying diseases such as hypertension, hyperlipidemia, and other risk factors such as smoking, in which atherosclerotic lesions occur in the endothelium of coronary arteries, causing progressive stenosis or obstruction in the lumen of the blood vessels, and ultimately resulting in ischemia, hypoxia, and necrosis of myocardial tissues[1]. Epidemiological studies have shown[2] that as many as 330 million people suffer from cardiovascular diseases in China, approximately 11.39 million of whom have CHD; this number is currently a significant public health problem in China. The cause of angina pectoris (AP) is mainly coronary artery atherosclerosis or thrombosis, resulting in a blood supply that does not meet the needs of the heart; myocardial ischemia; and hypoxia caused by paroxysmal chest pain and dyspnea, the leading site of pain in the posterior part of the sternum. Additionally, the blood supply can also radiate to the front of the chest and the ulnar side of the left upper limb[3]. Coronary angina pectoris usually occurs when the patient is emotionally agitated or overworked, and the disease can be relatively acute. If appropriate action is not taken promptly, the patient's condition will worsen gradually, putting their safety at risk. Timely treatment of patients suffering from AP can improve their clinical prognosis and reduce the likelihood of sudden death, myocardial infarction, and other adverse events, thereby improving overall health.

Guanxinjing capsule (GXJ) is a commonly used Chinese medicine compound preparation for the treatment of AP in CHD[4]. The formula consists of 9 Chinese medicines: Radix Salviae, Radix

ISSN 2706-6819 Vol.7, Issue 3: 1-16, DOI: 10.25236/IJFM.2025.070301

Paeoniae Rubra, Chuanxiong Rhizoma, and Panax notoginseng (Burk.) F. H. Chen Ex C. Chow, Carthami Flos, Styrax, Borneolum Syntheticum, Panax Ginseng C. A. Mey, and Polygonati Odorati Rhizoma, work together to activate blood circulation, remove blood stasis and promote circulation. Its apparent efficacy in treating AP has been confirmed in long-term clinical practice, as it can shorten the duration of angina attacks, and reduce the frequency of angina attacks. Clinical research has shown that GXJ is safe to administer, does not cause adverse reactions, and is one of the most commonly used medicines in Chinese medicine for the treatment of CHD[5-9]. GXJ has more flavors and complex compositions. Because traditional Chinese medicine involves multicomponent and multitarget regulation, its mechanism of action in the treatment of AP still needs to be determined. Conventional pharmacological studies mostly use animal or cellular methods to explore a single mechanism of action,and it is difficult to construct a network of drug action mechanisms from a holistic perspective.

Cyberpharmacology is based on the theories of systems biology, genomics, multidirectional pharmacology, proteomics, and other disciplines and uses technologies such as histology, high-throughput screening, and network visualization to reveal the complex biological network relationships between drugs, genes, targets, and diseases[10].Molecular docking is a simulation method for predicting the binding mode and affinity between two receptors and ligands by analyzing their property characteristics and interactions through an electric field. In the field of traditional Chinese medicine (TCM), molecular docking technology is used to dock small molecule active substances with relevant target proteins, to elucidate the pharmacological composition and mechanism of action of TCM at the molecular level. The combination of network pharmacology and molecular docking can reveal the relationships among molecules, targets, and diseases, providing a theoretical basis and technical support for studying the pharmacological mechanism of Chinese medicine compounds.

In this study, network pharmacology and molecular docking techniques were used to determine the targets of action for the main active ingredients of GXJ and the targets of action for AP in CHD. A network of GXJ component targets and a PPI network of chemical and disease interaction targets were constructed. The signaling pathways associated with biological function and efficacy were subsequently investigated using Gene Ontology (GO) and Kyoto Encyclopedia of Genes and Genomes (KEGG) enrichment analyses. Finally, the proposed functional components and main targets were validated via molecular docking techniques. The flow of the study is shown in Figure 1.

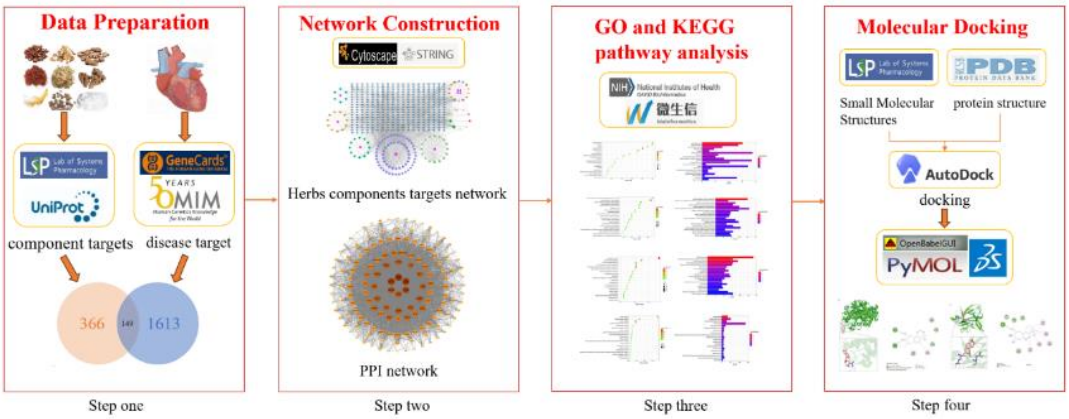

Figure 1 Workflow of the study design

2. Materials and Methods

2.1 Acquisition of Information on Relevant Active Ingredients and Corresponding Targets of GXJ

The active ingredients of Radix Salviae, Radix Paeoniae Rubra, Chuanxiong Rhizoma, and Panax notoginseng (Burk.) F. H. Chen Ex C. Chow, Carthami Flos, Styrax, Borneolum Syntheticum, Panax Ginseng C. A. Mey, and Polygonati Odorati Rhizoma were obtained from GXJ by searching the TCMSP database (http://tcmspw.com/tcmsp.php) and were screened for their active ingredients according to the criteria of oral bioavailability (OB) ≥30%, and drug Likeness (DL) ≥0.18. In the TCMSP, the Related Targets tag was utilized to fetch the targets of each active ingredient. The targets, chemical components, and corresponding Chinese medicine names were determined. To convert the names of target proteins to gene names, we referred to the UniProt database (http://www.UniProt.org/).

ISSN 2706-6819 Vol.7, Issue 3: 1-16, DOI: 10.25236/IJFM.2025.070301

2.2 Screening of Angina Pectoris Targets

The keyword "Angina Pectoris" was used to search the GeneCards (https://www.genecards.org/) database and OMIM database (https://omim.org/), and the results of the two searches were combined to determine the disease target of CHD. The Venn diagram shows the intersection of the drug constituent targets and disease targets.

2.3 Protein Interaction Network Analysis

The intersecting targets were imported into the STRING database (https://string-db.org/), the species "*Homo sapiens*" was selected, the confidence score was set to >0.4 (medium confidence), and the hidden protein interactions were selected. The intersecting target interaction network topology was constructed by setting the confidence score to >0.4 (medium confidence) and selecting Hide Disconnected Nodes in the Network (PPI Network), with the rest of the parameters set to default values. Using the CytoNCA plug-in of Cytoscape 3.10.1 software, topology analysis was performed to calculate the degree centrality (DC), closeness centrality (CC), and betweenness centrality (BC) of each node. First, the target genes with DC ≥ 2 times the median DC were screened, and second, the core target genes were obtained by screening with the criterion that "DC, BC, and CC are greater than or equal to their median."

2.4 Potential Targets of Action Compound Network Diagram Construction

Cytoscape 3.10.1 software was used to visualize and analyze the active ingredients and corresponding targets, and a compound network diagram of TCM-component-potential targets was constructed, in which the TCM, components and targets are represented by nodes, and the relationship between each node is represented by dotted lines.

2.5 GO Analysis and KEGG Pathway Analysis

The intersecting targets of GXJ for the treatment of AP in CHD were imported into the DAVID 6.8 database, and GO analysis and KEGG pathway enrichment analysis were carried out on the potential targets of biological process (BP), cellular component (CC), and molecular function (MF). When $P < 0.05$, the difference was considered statistically significant, the top 20 results were discussed and analyzed, and the enrichment analysis bar chart and enrichment analysis bubble chart were drawn with the use of bioinformatics.

2.6 Molecular Docking

Molecular docking is a theoretical simulation method used to study intermolecular interactions and predict their binding modes and affinities. In this study, the top 8 drug components were screened according to the network diagram of TCM compounds, 8 core targets were screened according to the PPI network for molecular docking, and the core components identified by the network pharmacology were verified to be bound to the core protein.

(1) First, the PDB files of the core proteins were collected and downloaded from the PDB database (http://www.rcsb.org/), after which the water and ligands were removed via PyMOL software. The proteins were assigned as receptors in AutoDock 4, after which the structures were saved as PDBQT protein receptor files.

(2) The mol2 format file of the drug molecule was downloaded from the TCMSP database, after which the drug was set as a ligand in AutoDock 4 and exported as a PDBQT format file.

(3) The receptor and ligand PDBQT structure files were imported into AutoDock 4, after which the molecular docking range was defined. With the target protein as the center of the grid, the center coordinates (center x/y/z) and the size of the docking frame (size x/y/z) were adjusted to ensure that the protein was completely covered by the docking box.

(4) The docking result with the lowest docking energy was selected and saved in PDBQT format. OpenBabelGUI software was used to convert the PDBQT format of the docking results into the PDB format. Finally, the results were analyzed and processed using PyMol 2.5 and Discovery Studio 2021.

ISSN 2706-6819 Vol.7, Issue 3: 1-16, DOI: 10.25236/IJFM.2025.070301

3. Results

3.1 Acquisition of Information on Relevant Active Ingredients and Corresponding Targets of GXJ

Table 1 All Chinese medicine ingredients collected from the TCMSP

Code	MOLID	Compound	OB	DL
A1	MOL001494	Mandenol	42	0.19
SQ02	MOL001792	DFV	32.76	0.18
B1	MOL002879	Diop	43.59	0.39
C1	MOL000358	beta-sitosterol	36.91	0.75
C2	MOL000449	Stigmasterol	43.83	0.76
B2	MOL005344	ginsenoside rh2	36.32	0.56
SQ07	MOL000098	quercetin	46.43	0.28
SQ08	MOL007475	ginsenoside f2	36.43	0.25
SHX01	MOL002039	Isopimaric acid	36.2	0.28
SHX02	MOL003790	Androstane	32.5	0.26
SHX03	MOL001663	(4aS,6aR,6aS,6bR,8aR,10R,12aR,14bS)-10-hydroxy-2,2,6a,6b,9,9,12a-heptamethyl-1,3,4,5,6,6a,7,8,8a,10,11,12,13,14b-tetradecahydropicene-4a-carboxylic acid	32.03	0.76
RS04	MOL003648	Inermin	65.83	0.54
RS05	MOL000422	kaempferol	41.88	0.24
RS06	MOL005308	Aposiopolamine	66.65	0.22
RS07	MOL005317	Deoxyharringtonine	39.27	0.81
RS08	MOL005318	Dianthramine	40.45	0.2
RS09	MOL005320	arachidonate	45.57	0.2
RS10	MOL005321	Frutinone A	65.9	0.34
RS12	MOL005348	Ginsenoside-Rh4_qt	31.11	0.78
RS13	MOL005356	Girinimbin	61.22	0.31
RS14	MOL005376	Panaxadiol	33.09	0.79
RS15	MOL005384	suchilactone	57.52	0.56
RS16	MOL005399	alexandrin_qt	36.91	0.75
RS17	MOL000787	Fumarine	59.26	0.83
RS18	MOL004492	Chrysanthemaxanthin	38.72	0.58
RS19	MOL005314	Celabenzine	101.88	0.49
RS20	MOL005357	Gomisin B	31.99	0.83
YZ01	MOL010395	4',5,7-trihydroxy-6-methyl-8-methoxy-homoisoflavanone	89.7	0.33
YZ02	MOL010396	4',5,7-trihydroxy-6,8-dimethyl-homoisoflavanone	59.76	0.3
YZ03	MOL010408	polygosides E_qt	38.73	0.78
YZ04	MOL010412	4'-methoxy-5,7-dihydroxy-6,8-dimethyl-homoisflavanone	57.14	0.34
YZ05	MOL000332	n-coumaroyltyramine	85.63	0.2
YZ06	MOL000483	(Z)-3-(4-hydroxy-3-methoxy-phenyl)-N-[2-(4-hydroxyphenyl)ethyl]acrylamide	118.35	0.26
BP01	MOL006865	dipterocarpol	41.71	0.76
BP02	MOL006861	asiatic acid	41.38	0.71

ISSN 2706-6819 Vol.7, Issue 3: 1-16, DOI: 10.25236/IJFM.2025.070301

DS01	MOL001601	1,2,5,6-tetrahydrotanshinone	38.75	0.36
DS02	MOL001659	Poriferasterol	43.83	0.76
D1	MOL001771	poriferast-5-en-3beta-ol	36.91	0.75
DS04	MOL001942	isoimperatorin	45.46	0.23
DS05	MOL002222	sugiol	36.11	0.28
DS06	MOL002651	Dehydrotanshinone II A	43.76	0.4
E1	MOL002776	Baicalin	40.12	0.75
DS08	MOL000569	digallate	61.85	0.26
DS09	MOL000006	luteolin	36.16	0.25
DS10	MOL007036	5,6-dihydroxy-7-isopropyl-1,1-dimethyl-2,3-dihydrophenanthren-4-one	33.77	0.29
DS11	MOL007041	2-isopropyl-8-methylphenanthrene-3,4-dione	40.86	0.23
DS12	MOL007045	3α-hydroxytanshinoneIIa	44.93	0.44
DS13	MOL007048	(E)-3-[2-(3,4-dihydroxyphenyl)-7-hydroxy-benzofuran-4-yl]acrylic acid	48.24	0.31
DS14	MOL007049	4-methylenemiltirone	34.35	0.23
DS15	MOL007050	2-(4-hydroxy-3-methoxyphenyl)-5-(3-hydroxypropyl)-7-methoxy-3-benzofurancarboxaldehyde	62.78	0.4
DS16	MOL007058	formyltanshinone	73.44	0.42
DS17	MOL007059	3-beta-Hydroxymethyllenetanshiquinone	32.16	0.41
DS18	MOL007061	Methylenetanshinquinone	37.07	0.36
DS19	MOL007063	przewalskin a	37.11	0.65
DS20	MOL007064	przewalskin b	110.32	0.44
DS21	MOL007068	Przewaquinone B	62.24	0.41
DS22	MOL007069	przewaquinone c	55.74	0.4
DS23	MOL007070	(6S,7R)-6,7-dihydroxy-1,6-dimethyl-8,9-dihydro-7H-naphtho[8,7-g]benzofuran - 10,11-dione	41.31	0.45
DS24	MOL007071	przewaquinone f	40.31	0.46
DS25	MOL007077	sclareol	43.67	0.21
DS26	MOL007079	tanshinaldehyde	52.47	0.45
DS27	MOL007081	Danshenol B	57.95	0.56
DS28	MOL007082	Danshenol A	56.97	0.52
DS29	MOL007085	Salvilenone	30.38	0.38
DS30	MOL007088	cryptotanshinone	52.34	0.4
DS31	MOL007093	dan-shexinkum d	38.88	0.55
DS32	MOL007094	danshenspiroketallactone	50.43	0.31
DS33	MOL007098	deoxyneocryptotanshinone	49.4	0.29
DS34	MOL007100	dihydrotanshinlactone	38.68	0.32
DS35	MOL007101	dihydrotanshinoneI	45.04	0.36
DS36	MOL007105	epidanshenspiroketallactone	68.27	0.31
DS37	MOL007107	C09092	36.07	0.25
DS38	MOL007108	isocryptotanshi-none	54.98	0.39
DS39	MOL007111	Isotanshinone II	49.92	0.4
DS40	MOL007115	manool	45.04	0.2

ISSN 2706-6819 Vol.7, Issue 3: 1-16, DOI: 10.25236/IJFM.2025.070301

DS41	MOL007118	microstegiol	39.61	0.28
DS42	MOL007119	miltionone I	49.68	0.32
DS43	MOL007120	miltionone II	71.03	0.44
DS44	MOL007121	miltipolone	36.56	0.37
DS45	MOL007122	Miltirone	38.76	0.25
DS46	MOL007124	neocryptotanshinone ii	39.46	0.23
DS47	MOL007125	neocryptotanshinone	52.49	0.32
DS48	MOL007127	1-methyl-8,9-dihydro-7H-naphtho[5,6-g]benzofuran-6,10,11-trione	34.72	0.37
DS49	MOL007130	prolithospermic acid	64.37	0.31
DS50	MOL007132	(2R)-3-(3,4-dihydroxyphenyl)-2-[(Z)-3-(3,4-dihydroxyphenyl)acryloyl]oxy-propionic acid	109.38	0.35
DS51	MOL007140	(Z)-3-[2-[(E)-2-(3,4-dihydroxyphenyl)vinyl]-3,4-dihydroxy-phenyl]acrylic acid	88.54	0.26
DS52	MOL007141	salvianolic acid g	45.56	0.61
DS53	MOL007142	salvianolic acid j	43.38	0.72
DS54	MOL007143	salvilenone I	32.43	0.23
DS55	MOL007145	salviolone	31.72	0.24
DS56	MOL007149	NSC 122421	34.49	0.28
DS57	MOL007150	(6S)-6-hydroxy-1-methyl-6-methylol-8,9-dihydro-7H-naphtho[8,7-g]benzofuran- 10,11-quinone	75.39	0.46
DS58	MOL007151	Tanshindiol B	42.67	0.45
DS59	MOL007152	Przewaquinone E	42.85	0.45
DS60	MOL007154	tanshinone iia	49.89	0.4
DS61	MOL007155	(6S)-6-(hydroxymethyl)-1,6-dimethyl-8,9-dihydro-7H-naphtho[8,7-g]benzofuran-10,11-dione	65.26	0.45
DS62	MOL007156	tanshinone VI	45.64	0.3
CS01	MOL002883	Ethyl oleate (NF)	32.4	0.19
F1	MOL002714	baicalein	33.52	0.21
CS03	MOL000492	(+)-catechin	54.83	0.24
CS04	MOL006992	(2R,3R)-4-methoxyl-distylin	59.98	0.3
CS05	MOL001918	paeoniflorgenone	87.59	0.37
CS06	MOL001002	ellagic acid	43.06	0.43
CS07	MOL005043	campest-5-en-3beta-ol	37.58	0.71
CS08	MOL006999	stigmast-7-en-3-ol	37.42	0.75
G1	MOL000359	sitosterol	36.91	0.75
CS12	MOL004355	Spinasterol	42.98	0.76
CS14	MOL001924	paeoniflorin	53.87	0.79
CS15	MOL001921	Lactiflorin	49.12	0.8
CS16	MOL007004	Albiflorin	30.25	0.77
CS17	MOL007016	Paeoniflorigenone	65.33	0.37
CX02	MOL002135	Myricanone	40.6	0.51
CX03	MOL002140	Perlolyrine	65.95	0.27
CX04	MOL002157	wallichilide	42.31	0.71

ISSN 2706-6819 Vol.7, Issue 3: 1-16, DOI: 10.25236/IJFM.2025.070301

CX06	MOL000433	FA	68.96	0.71
CX07	MOL002151	senkyunone	47.66	0.24
HH02	MOL002694	4-[(E)-4-(3,5-dimethoxy-4-oxo-1-cyclohexa-2,5-dienylidene)but-2-enylidene]-2,6-dimethoxycyclohexa-2,5-dien-1-one	48.47	0.36
HH03	MOL002695	lignan	43.32	0.65
HH04	MOL002710	Pyrethrin II	48.36	0.35
HH05	MOL002712	6-Hydroxykaempferol	62.13	0.27
HH07	MOL002717	qt_carthamone	51.03	0.2
HH08	MOL002721	quercetagetin	45.01	0.31
HH09	MOL002757	7,8-dimethyl-1H-pyrimido[5,6-g]quinoxaline-2,4-dione	45.75	0.19
HH10	MOL002773	beta-carotene	37.18	0.58
HH11	MOL002680	Flavoxanthin	60.41	0.56
HH12	MOL002698	lupeol-palmitate	33.98	0.32
HH13	MOL002719	6-Hydroxynaringenin	33.23	0.24

Based on the characteristics of multiple constituents and multiple targets of TCM, we obtained the active ingredients of the drug GXJ by searching the TCMSP database. The 127 active ingredients met the screening criteria (OB≥30%, DL≥0.18), as shown in Table 1.

3.2 Screening of Angina Disease Targets

Using "Angina Pectoris" as the keyword, 1510 related disease targets were obtained from the GeneCards (https://www.genecards.org/) database, 141 related targets were obtained from the OMIM database, and after excluding duplicate genes, we obtained 1613 targets related to AP in CHD.

The 366 drug targets of the GXJ capsule and the 1613 disease targets of AP were matched to determine the intersection, and 149 shared genes were obtained; these genes were the potential targets of action of the GXJ capsule for the treatment of AP (see Fig. 2).

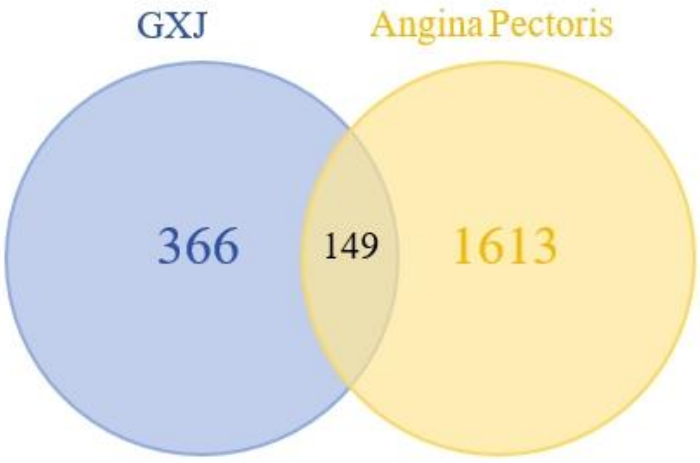

Figure 2 Venn diagram of GXJ targets and AP disease-related targets

3.3 Potential Targets of Action Compound Network Diagram Construction

Cytoscape 3.10.1 software was used to construct the herbal medicine-ingredient-potential action target complex network, which included 503 nodes, and 127 active ingredients such as beta-sitosterol, quercetin, and baicalein; 366 drug targets such as human phosphatidylinositol-3-kinase catalytic subunit G peptide (PIK3CG) and tumor necrosis factor (TNF); and 366 other drug targets, connected by 2061 edges (see Figure 3).

ISSN 2706-6819 Vol.7, Issue 3: 1-16, DOI: 10.25236/IJFM.2025.070301

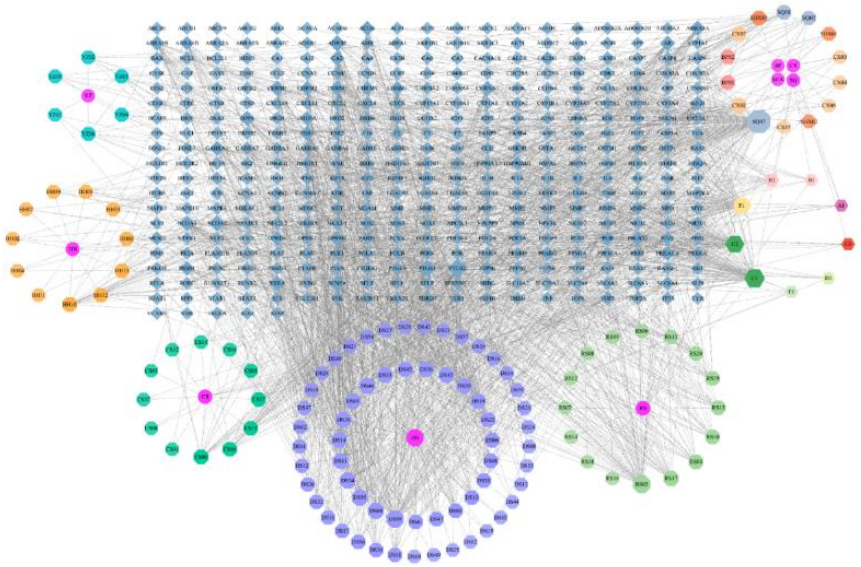

Figure 3 The herbal medicine-ingredient-potential action target network diagram

A1 indicates that Mandenol, a shared constituent of Panax notoginseng (Burk.) F. H. Chen Ex C. Chow and Chuanxiong Rhizoma; B1 indicates Diop, a shared constituent of Panax notoginseng (Burk.) F. H. Chen Ex C. Chow and Panax Ginseng C. A. Mey; B2 indicates ginsenoside rh2, a shared constituent of Panax notoginseng (Burk.) F. H. Chen Ex C. Chow and Panax Ginseng C. A. Mey; C1 indicates beta-sitosterol, a shared constituent of Panax notoginseng (Burk.) F. H. Chen Ex C. Chow, Panax Ginseng C. A. Mey, and Radix Paeoniae Rubra; C2 indicates stigmasterol, a shared constituent of Panax notoginseng (Burk.) F. H. Chen Ex C. Chow, Panax Ginseng C. A. Mey and Radix Paeoniae Rubra; D1 indicates poriferous-5-en-3beta-ol, a shared constituent of Radix Salviae and Carthami Flos; E1 indicates baicalin, a shared constituent of Radix Salviae and Radix Paeoniae Rubra; F1 indicates baicalein, a shared constituent of Radix Paeoniae Rubra and Carthami Flos; G1 indicates baicalein, a shared constituent of Radix Paeoniae Rubra and Chuanxiong Rhizoma.

3.4 PPI Network Construction and Analysis

To investigate whether there were protein interactions among the intersecting genes, we constructed a PPI network through the STRING network platform. The protein interaction network analysis revealed that there were 149 targets connected through 3604 edges. The analysis identified eight key targets, namely, IL6, TNF, ESR1, AKT1, IL1B, MMP9, PPARG, and TP53. A PPI network was created based on the analysis, and the node colour depth represents the connectivity level. The results are visualized in Fig4.

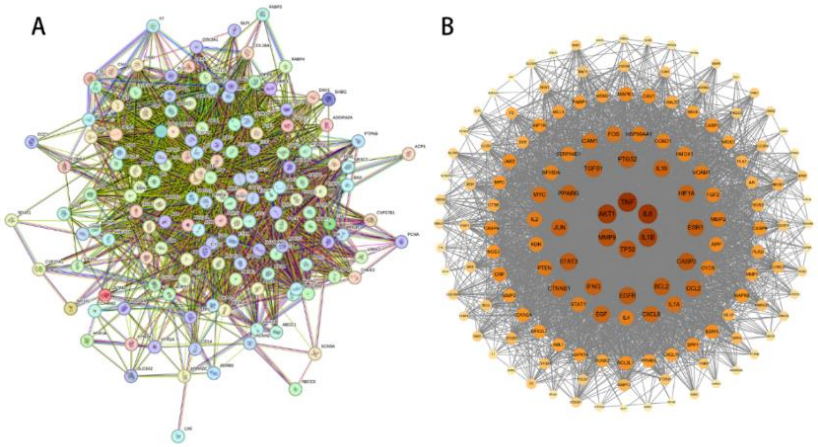

Figure 4 (A)PPI network diagram of candidate genes (B) Topological analysis diagram of the candidate genes

ISSN 2706-6819 Vol.7, Issue 3: 1-16, DOI: 10.25236/IJFM.2025.070301

3.5 GO Analysis and KEGG Pathway Analysis

3.5.1 GO Analysis

The potential targets for the treatment of AP in CHD with GXJ were imported into the DAVID 6.8 database, and GO enrichment analysis was carried out on 149 potential targets, resulting in a total of 1,129 relevant pathways, of which 877 were involved in biological process (BP) pathways, 102 were involved in cellular component (CC) pathways, and 150 were involved in molecular function (MF) pathways. The top 20 pathways were sorted by P value, and the enrichment analysis bar chart and enrichment analysis bubble chart were drawn by bioinformatics. Fig5 shows that the BP terms were involved in the positive regulation of gene expression, the positive regulation of pri-miRNA transcription from the RNA polymerase II promoter, response to xenobiotic stimulus, positive regulation of protein phosphorylation, positive regulation of cell proliferation, positive regulation of transcription from the RNA polymerase II promoter, negative regulation of the apoptotic process, response to hypoxia stimulus, positive regulation of angiogenesis, response to lipopolysaccharide, positive regulation of smooth muscle cell proliferation, inflammatory response, apoptotic process, positive regulation of MAP kinase activity, negative regulation of gene expression, positive regulation of transcription, DNA-templated, positive regulation of nitric oxide biosynthetic process, positive regulation of apoptotic process, cellular response to lipopolysaccharide, and positive regulation of cell migration.

The top 20 signaling pathways in the GO-CC section included extracellular space, extracellular region, macromolecular complex, membrane raft, caveola, plasma membrane, cell surface, external side of plasma membrane, integral component of plasma membrane, cytoplasm, extracellular exosome, serine-type endopeptidase complex, cytosol, focal adhesion, RNA polymerase II transcription factor complex, ficolin-1-rich granule lumen, perinuclear region of cytoplasm, caspase complex, nucleoplasm, and receptor complex (see Fig5).

The top 20 signaling pathways in the GO-MF section included enzyme binding, identical protein binding, protein homodimerization activity, protein binding, protein kinase binding,serine-type endopeptidase activity, cytokine activity, endopeptidase activity, RNA polymerase II transcription factor activity, ligand-activated sequence-specific DNA binding, ubiquitin protein ligase binding, integrin binding, protease binding, heme binding, protein phosphatase binding, receptor binding, growth factor activity, peptidase activity, RNA polymerase II sequence-specific DNA binding transcription factor binding, protein serine/threonine/tyrosine kinase activity, and steroid binding (see Fig6).

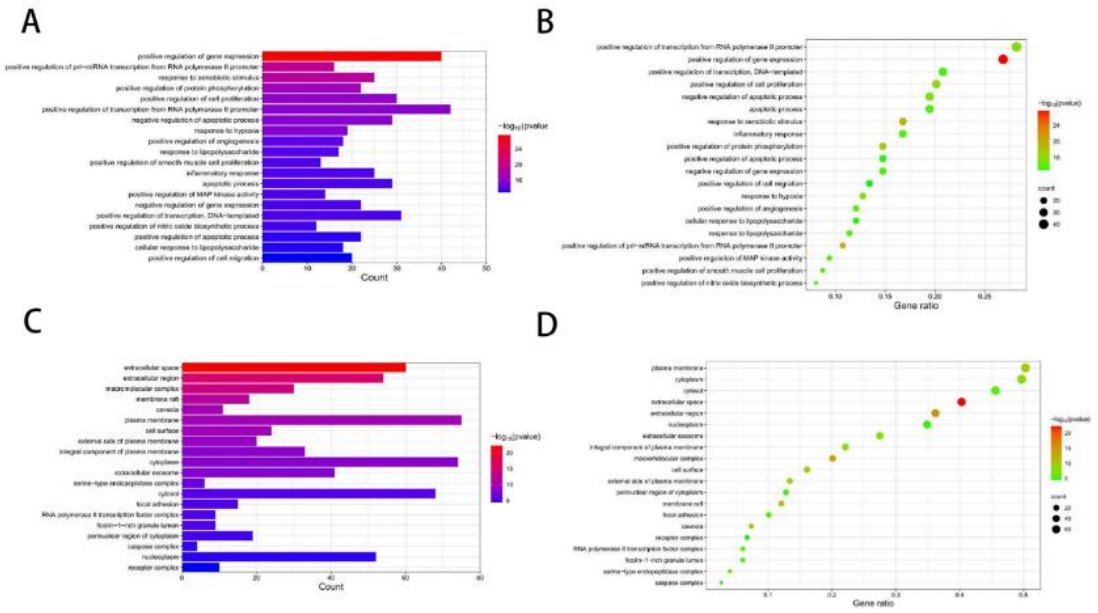

Figure 5 (A) GO-BP enrichment analysis bar chart. (B) GO-BP enrichment analysis bubble chart. (C) GO-CC enrichment analysis bar chart. (D) CC enrichment analysis bubble chart.

ISSN 2706-6819 Vol.7, Issue 3: 1-16, DOI: 10.25236/IJFM.2025.070301

3.5.2 KEGG Pathway Enrichment Analysis

KEGG enrichment analysis revealed that a total of 96 relevant pathways were involved in the treatment of CHD-related angina pectoris with GXJ, of which the top 20 signaling pathways included pathways associated with cancer, the AGE-RAGE signaling pathway associated with diabetic complications, lipids and atherosclerosis, fluid shear stress and atherosclerosis, Kaposi sarcoma-associated herpesvirus infection, toxoplasmosis, the IL-17 signaling pathway, hepatitis B, prostate cancer, proteoglycans in cancer, human cytomegalovirus infection, the TNF signaling pathway, leishmaniasis, EGFR tyrosine kinase inhibitor resistance, tuberculosis, colorectal cancer, Chagas disease, bladder cancer, chemical carcinogenesis-receptor activation, and the PI3K-Akt signaling pathway (see Fig6).

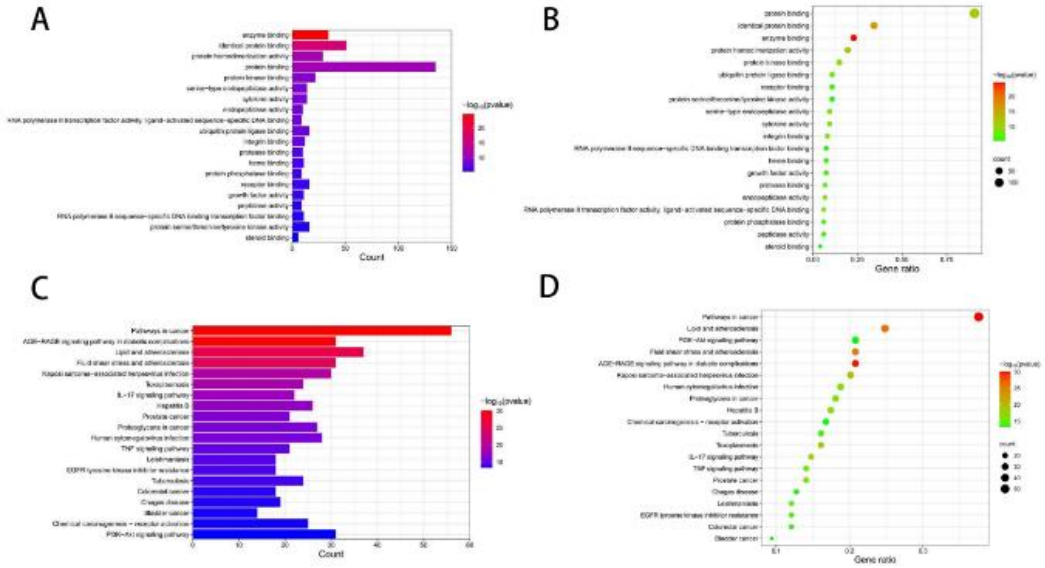

Figure 6 (A) GO-MF enrichment analysis bar chart. (B) GO-MF enrichment analysis bubble chart. (C) KEGG enrichment analysis bar chart. (D) KEGG enrichment analysis bubble chart.

3.6 Analysis of the Molecular Docking Results

Based on the results of the network pharmacology study, we screened the top 8 drug components beta-sitosterol, quercetin, stigmasterol, baicalein, kaempferol, luteolin, tanshinone IIA, and salviolone, and the top 8 ranked targets were IL6 (PDB ID: 7JRA), TNF (PDB ID: 5WJJ), ESR1 (PDB ID: 3L03), AKT1 (PDB ID: 4EJN), IL1B (PDB ID: 1T4Q), MMP9 (PDB ID: 5CUH), PPARG (PDB ID: 5Y2T), and TP53 (PDB ID: 6VA5). These components and genes were subjected to molecular docking, and the docking results of the drug components and proteins are shown in Fig 7. We selected the docking results of the top 10 binding activities for visualization, and the visualized 3D and 2D images are shown in Fig7.

As shown in Fig7-1A, salviolone can form a hydrogen bond with MET-20 and GLN-38 in 2NVH, and Fig7-1B shows that salviolone can form a hydrogen bond with ASP-332 in 3L03. Fig7-2C shows that beta-sitosterol can form a hydrogen bond with MET-247 in 5CUH. Fig7-2D shows that quercetin can form one hydrogen bond with ARG-249, GLU-227, MET-247, or ALA-242 at 5CUH. Fig7-3E shows that salviolone can form one hydrogen bond with each of MET-247 and LEU-243 in 5CUH and two hydrogen bonds with ARG-249. Fig7-3F shows that tanshinone IIA can form one hydrogen bond with each of LEU-222 and TYR-245 in 5CUH and two hydrogen bonds with MET-247. Fig7-4G shows that stigmasterol can form one hydrogen bond with GLU-130 at 5CUH. Fig7-4H shows that beta-sitosterol can form one hydrogen bond with 5WJJ in GLY-85 and THR-106.

It is generally accepted that when the binding energy of a ligand to a receptor is lower, the binding conformation is more stable, and the possibility of interaction is greater. A binding energy < 0 kcal/mol indicates that the receptor and ligand can bind in the natural state, and a binding energy < -5 kcal/mol suggests that the ligand and receptor have excellent binding activity. The present docking results showed that the binding energies of only 10 out of the 64 docking products were greater than -5

ISSN 2706-6819 Vol.7, Issue 3: 1-16, DOI: 10.25236/IJFM.2025.070301

kcal/mol (5Y2T-quercetin, 2NVH-quercetin, 5Y2T-kaempferol, 5Y2T-baicalein, 7JRA-quercetin, 3L03-luteolin, 3L03-kaempferol, 2NVH-kaempferol, 4EJN-kaempferol, and 3L03-quercetin), and the binding energies of all the products were less than 0 kcal/mol, indicating that the core drug components bind well to the critical target proteins. Therefore, the core components predicted in this study may play a vital role in the treatment of AP in CHD by acting on target proteins such as MMP9, TNF, IL1B, TP53, and ESR1.

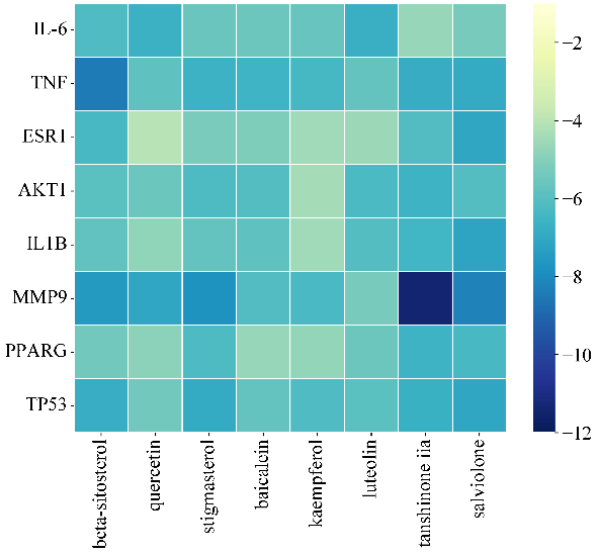

Figure 7 Heat map of molecular docking results

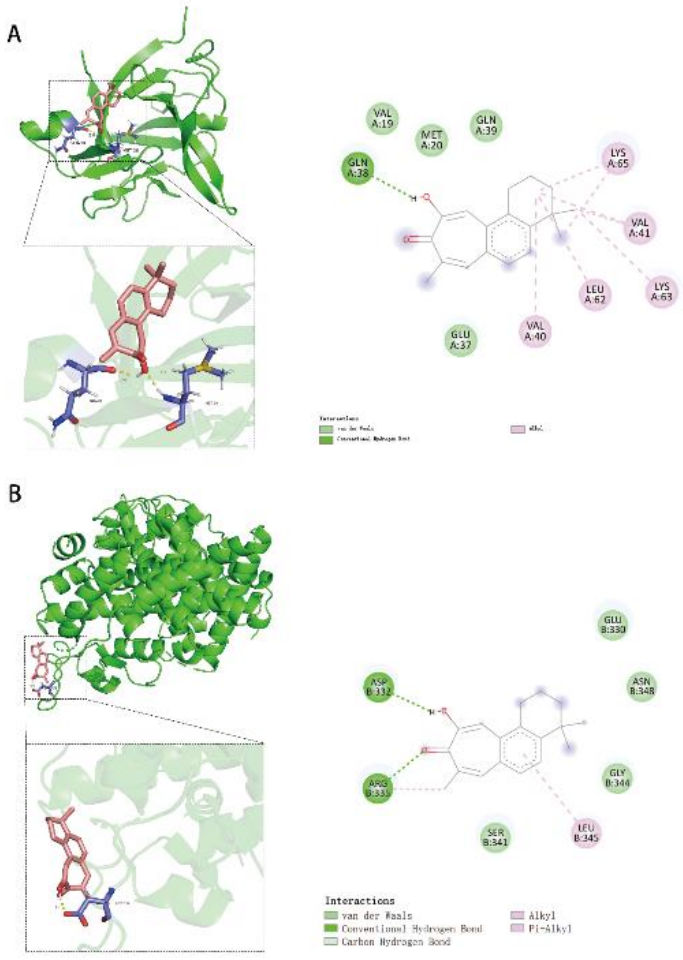

Figure 7-1 Molecular docking diagrams. (A) IL1B-Salviolone, (B) ESR1-salviolone

ISSN 2706-6819 Vol.7, Issue 3: 1-16, DOI: 10.25236/IJFM.2025.070301

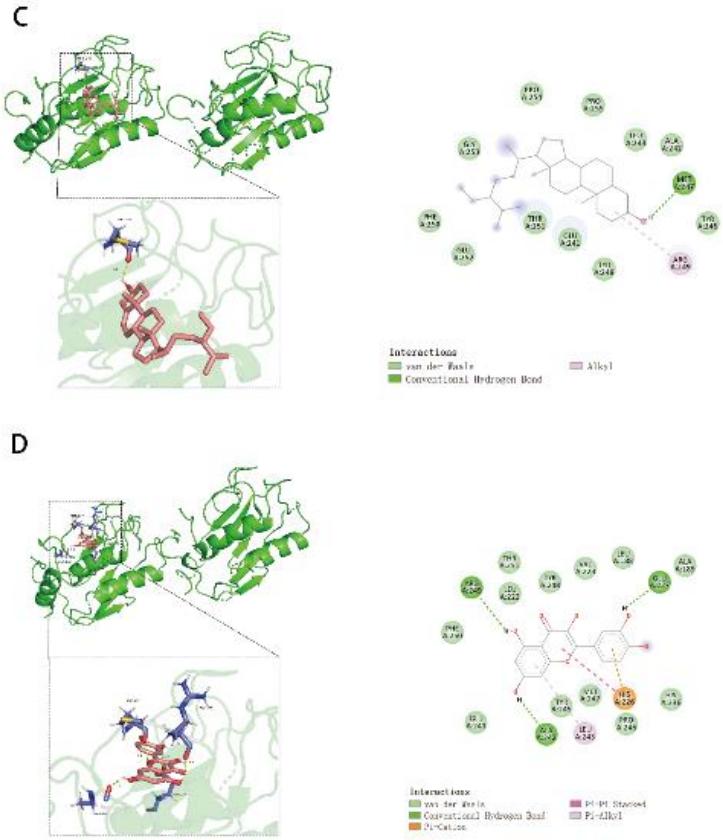

Figure 7-2 Molecular docking diagrams. (C) MMP9-beta-sitosterol, (D) MMP9-quercetin

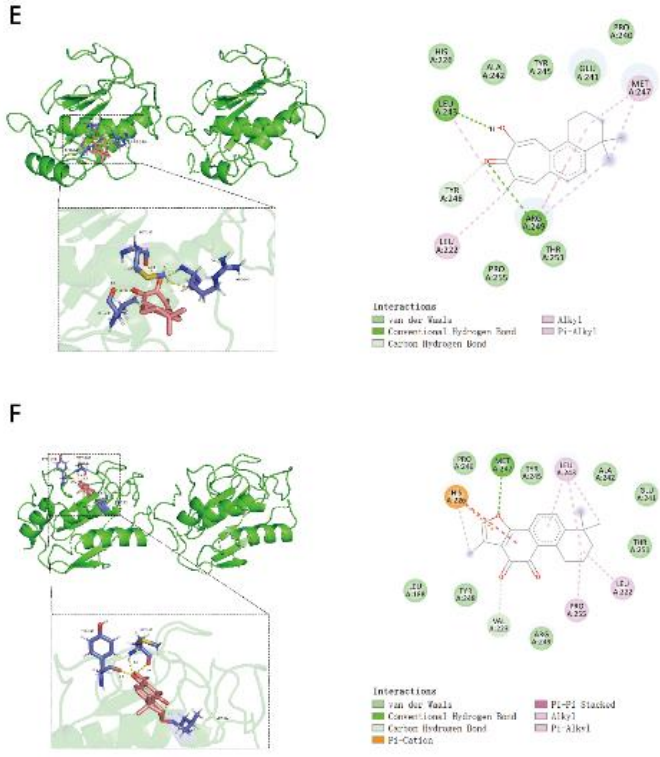

Figure 7-3 Molecular docking diagrams. (E) MMP9-salviolone, (F) MMP9-tanshinone iia

ISSN 2706-6819 Vol.7, Issue 3: 1-16, DOI: 10.25236/IJFM.2025.070301

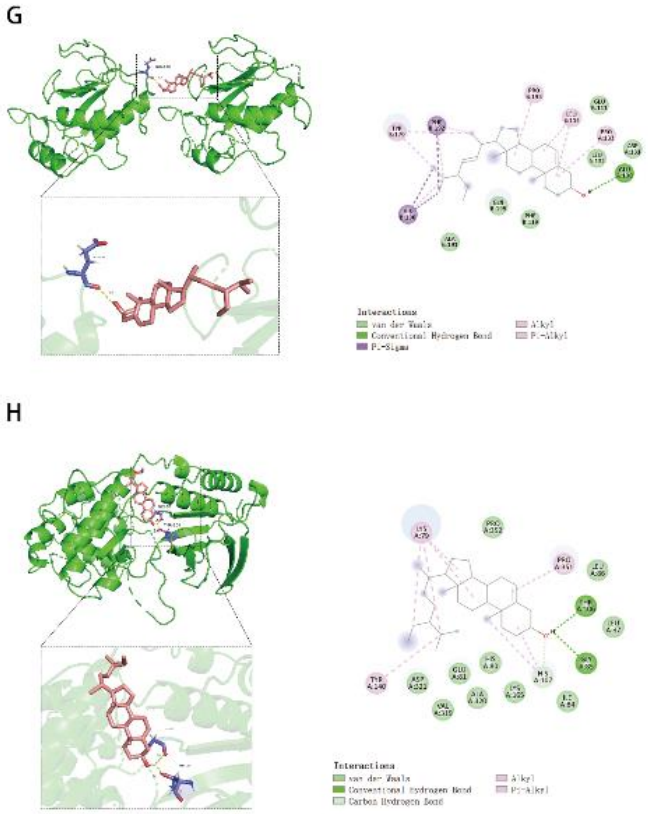

Figure 7-4 Molecular docking diagrams. (G) MMP9-stigmasterol, (H) TNF-beta-sitosterol.

4. Discussion

Angina pectoris is a common cardiovascular disease that is caused primarily by emotional excitement and overwork. The onset of more acute, if not timely and effective interventions, seriously affect patient's life and health. In recent years, the incidence of CHD-related angina pectoris in China has been increasing annually, and CHD-related angina pectoris patients are being diagnosed at younger ages. Therefore, it is essential to explore effective treatment methods and drugs actively. With the in-depth study of Chinese medicine clinics, Chinese medicine treatment for AP has become diverse, and all kinds of therapies have achieved good efficacy.

GXJ is a commonly used herbal compound preparation for the clinical treatment of AP in CHD. However, the bioactive compounds of GXJ for the treatment of AP in CHD and their underlying mechanisms have yet to be investigated. Therefore, the present study used network pharmacology and molecular docking analyses to determine the potential targets and mechanisms of GXJ for the treatment of AP.

In this study, 127 active components of GXJ with corresponding targets were screened from the TCMSP database, and the first eight active compounds, β-sitosterol, quercetin, stigmasterol, baicalin, kaempferol, lignoceroside, tanshinone IIA, and rhamnolone, may be potential active components of GXJ for the treatment of AP in CHD. It was found[11] that the Chinese herb yam containing β-sitosterol reduced the area of aortic atherosclerotic lesions in ApoE (-/-) mice by affecting the expression of inflammatory mediators and lowering total cholesterol, oxidized low-density lipoproteins, and C-reactive protein levels in the mice, which in turn affected atherosclerosis. Quercetin can regulate the formation of acute coronary thrombosis and antiplatelet aggregation and plays a role in the treatment of CHD[12]. Soya sterol is a phytosterol that has antioxidative stress, lipid-lowering, and blood glucose-regulating effects[13]. Baicalin can alleviate oxidative damage by stabilizing MARCH5 levels in cells and tissues, regulating the KLF4-MARCH5-Drp1 pathway, and alleviating I/R stress, thus attenuating apoptosis to protect cardiomyocytes[14]. Chinese medicines containing kaempferol inhibit

ISSN 2706-6819 Vol.7, Issue 3: 1-16, DOI: 10.25236/IJFM.2025.070301

adriamycin-induced cardiotoxicity via the AKT/Bcl-2 signaling pathway[15]. Lignans are a class of flavonoids that have been shown to protect against I/R-induced cardiac injury by upregulating the antioxidant effects of NRF2[16] and inhibiting inflammatory cytokines[17]. Tanshinone IIA reduces vascular endothelial inflammation and prevents atherosclerotic plaque formation through the COX-2/TNF-α/NF-κB signaling pathway[18]. Sage phenolone has many pharmacological effects, such as antiradical, antioxidant, and anticancer effects, and it inhibits cancer cell migration and invasion[19]. These findings suggest that the active ingredient in GXJ has a favorable therapeutic effect on AP in CHD.

In this study, we retrieved AP targets through the GeneCards database and OMIM database. We identified 149 common targets between AP targets and GXJ drug component targets using a Venn diagram. These targets are considered potential targets of GXJ for the treatment of AP. To explore the core targets, we constructed a PPI network through the STRING network platform. The results showed that IL6, TNF, ESR1, AKT1, IL1B, MMP9, PPARG, and TP53 might be the core targets. IL6 is a key cytokine for innate immunity and a biomarker for vascular risk. IL6 promotes thrombosis and aneurysm formation in atherosclerosis[20]. TNF mediates endothelial adhesion molecules and proinflammatory factors in human and mouse atherosclerosis[21]. High expression of ESR1 can improve biochemical indices, such as MCP-1, TNF-β, and IL-6, in patients with CHD and effectively reduce the formation of macrophage foam cells, which are anti-inflammatory agents[22]. AKT1 can inhibit the proliferation, migration, and invasion of vascular smooth muscle cells and human umbilical vein endothelial cells and plays an important role in atherosclerosis[15]. IL1B has been proven to induce endothelial cell proliferation, migration, and invasion in atherogenesis and aneurysm formation in humans and mice. Sclerosis can induce an inflammatory response in endothelial cells, promote the aggregation and infiltration of immune cells in the vascular endothelium, and stimulate the proliferation and differentiation of vascular smooth muscle[23]. MMP9 is a protein hydrolase that contains zinc ions and is the most abundant enzyme in cardiomyocytes. The increased expression of MMP9 may have a certain predictive value for the stability of plaque lesions. MMP9 can degrade the fibrous cap of vulnerable plaques, which can cause the plaque's fibrous cap to thinen, increasing plaque instability, leading to plaque rupture vulnerability, and accelerating thrombosis[24]. PPARG activates the PPAR-γ/Nrf2 pathway by increasing PPARG expression, which reduces the myocardial infarction area, improves cardiac function, and plays a cardioprotective role[25]. In addition, increased PPARG expression can delay the progression of atherosclerotic plaques[26]. TP53 plays an important role in a variety of biological processes. During I/R, elevated levels of TP53 cause accelerated cardiac injury, whereas cardiac injury is reduced in TP53-deficient mice. Studies have shown that TP53 deficiency causes reduced oxidative stress, activation of calpain, and protection of mitochondria[27].

To explore the mechanism of action of GXJ in the treatment of AP in CHD, we performed GO analysis and KEGG enrichment analysis. The GO results revealed that these target genes were involved in biological functions such as negative regulation of apoptosis, positive regulation of angiogenesis, positive regulation of smooth muscle cell proliferation, inflammation, and positive regulation of nitric oxide biosynthesis. The results of the KEGG enrichment analysis suggested that the treatment of AP with GXJ involves multiple signaling pathways, including the IL-17 signaling pathway, TNF signaling pathway, PI3K-Akt signaling pathway, and PI3K-Akt signaling pathway. AP involves multiple signaling pathways, mainly the IL-17 signaling pathway, TNF signaling pathway, and PI3K-Akt signaling pathway. Apoptosis is a highly regulated process, and even a small amount of cardiomyocyte apoptosis may have serious consequences. Reducing the amount of cardiomyocyte apoptosis in I/R results in less cardiac injury[28]. It has been shown that IL-17 induces cardiomyocyte apoptosis, promotes myocardial tissue fibrosis, and polarizes macrophages to a pro-inflammatory phenotype after myocardial ischemia-reperfusion injury[29]. The TNF signaling pathway can induce cardiomyocyte apoptosis and myocardial tissue injury[30]. Modulation of the PI3K-Akt signaling pathway can intervene in cardiomyocyte inflammation and prevent apoptosis[31]. These findings demonstrate the potential of GXJ as an herbal compound for the treatment of AP in CHD.

To explore the potential molecular mechanism of GXJ in the treatment of AP-related CHD, based on the results of the above network pharmacological studies, i.e., the screening results of the active ingredients in the Chinese medicine compound and the screening results of the targets in the PPI network, we screened the top 8 active ingredients of the drug with the highest degree and the top 8 target-associated proteins. These eight compounds, beta-sitosterol, quercetin, stigmasterol, baicalein, kaempferol, luteolin, tanshinone IIA, and salviolone, were associated with IL6, TNF, ESR1, AKT1, IL1B, MMP9, PPARG, and TP53 according to molecular docking to validate our network pharmacological prediction results. The docking results showed that these eight core components had suitable binding activities with core proteins, indicating that their conformations were more stable and

ISSN 2706-6819 Vol.7, Issue 3: 1-16, DOI: 10.25236/IJFM.2025.070301

could form stable hydrogen bonds and hydrophobic interactions. Therefore, the core components predicted in this study may play a vital role in the treatment of AP in CHD by acting on target proteins such as IL6, TNF, ESR1, AKT1, IL1B, MMP9, PPARG, and TP53.

References

[1] Y Liu, Geng H-J, Cui X, et al. Clinical comprehensive evaluation of breviscapine injection in treatment of acute cerebral infarction and angina pectoris in coronary heart disease[J]. Chinese traditonal and herbal drugs, 2023, 54(19): 6413-6423.
[2] China-Cardiovascular-Health-And Group. Report on cardiovascular health and diseases in China 2022:an updated summary[J]. Chinese circulation journal, 2023, 38(06): 583-612.
[3] H-J Li, LIU X-Y, Li Z-L, et al. Research progress of therapy of Chinese medicine in treating angina pectoris of coronary heart disease[J]. Journal of Changchun university of Chinese, 2023, 39(11): 1280-1285.
[4] G-H Zhang, Jiang W-J, Zuo W-F, et al. Construction of the regulation network of "component-target-biological process and pathway" in Guanxinjing capsule in the treatment of coronary heart disease[J]. Journal of Shenyang pharmaceutical university, 2020, 37(06): 542-548.
[5] Y-L Dai, Bai H-R. Clinical study on Guanxinjing capsule in treating angina pectoris of Qi deficiency and blood stasis type[J]. Contemporary medicine, 2021, 27(22): 28-30.
[6] X-Y Li. Observation on curative effect of Guanxinjing capsule in treating coronary heart disease and angina pectoris due to qi deficiency and blood stasis[J]. Contemporary medicine, 2018, 24(34): 48-50.
[7] H-J Fan. Observation of the efficacy of Guanxinjing Capsule in the treatment of qi deficiency and blood stasis type coronary heart disease angina pectoris[J]. Chinese journal of integrative medicine on cardio-cerebrovascular disease, 2017, 15(06): 751-754.
[8] H-B Wang, Zhang T-H, Zhang X-B. Clinical efficacy and economic evaluation of Guanxinjing capsule for angina pectoris of coronary heart disease[J]. Chinese journal of drug evaluation, 2017, 34(01): 62-66.
[9] H-J Fan, Li S-R, Kang K-N, et al. Clinical observation of Guanxinjing capsules in treatment of stable exertional angina pectoris[J]. Drugs&Clinic, 2016, 31(07): 1016-1019.
[10] X Li, Wei S, Niu S, et al. Network pharmacology prediction and molecular docking-based strategy to explore the potential mechanism of Huanglian Jiedu Decoction against sepsis[J]. Comput Biol Med, 2022, 144105389.
[11] H-J Koo, Park H-J, Byeon H-E, et al. Chinese yam extracts containing beta-sitosterol and ethyl linoleate protect against atherosclerosis in apolipoprotein E-deficient mice and inhibit muscular expression of VCAM-1 in vitro[J]. J Food Sci, 2014, 79(4): H719-H729.
[12] Joana-Varlla de Lacerda Alexandre, Viana Yuana-Ivia-Ponte, David C ćera-Edna-Barbosa, et al. Quercetin treatment increases H2O2 removal by restoration of endogenous antioxidant activity and blocks isoproterenol-induced cardiac hypertrophy[J]. Naunyn-Schmiedeberg's Archives of Pharmacology, 2021, 394(2): 217-226.
[13] S Wang, Sun Y, Li C-M, et al. Research progress of stigmasterol[J]. China pharmaceuticals, 2019, 28(23): 96-98.
[14] Q Li, Yu Z, Xiao D, et al. Baicalein inhibits mitochondrial apoptosis induced by oxidative stress in cardiomyocytes by stabilizing MARCH5 expression[J]. J Cell Mol Med, 2020, 24(2): 2040-2051.
[15] Y Zhang, Liu S, Ma J-L, et al. Apocynum venetum leaf extract alleviated doxorubicin-induced cardiotoxicity through the AKT/Bcl-2 signaling pathway[J]. Phytomedicine, 2022, 94153815.
[16] I Andreadou, Iliodromitis E-K, Lazou A, et al. Effect of hypercholesterolaemia on myocardial function, ischaemia-reperfusion injury and cardioprotection by preconditioning, postconditioning and remote conditioning[J]. Br J Pharmacol, 2017, 174(12): 1555-1569.
[17] L Zhao, Zhou Z, Zhu C, et al. Luteolin alleviates myocardial ischemia reperfusion injury in rats via Siti1/NLRP3/NF-kappaB pathway[J]. Int Immunopharmacol, 2020, 85106680.
[18] X Ma, Zhang L, Gao F, et al. Salvia miltiorrhiza and Tanshinone IIA reduce endothelial inflammation and atherosclerotic plaque formation through inhibiting COX-2[J]. Biomed Pharmacother, 2023, 167115501.
[19] Y Yang, Cao Y, Chen L, et al. Cryptotanshinone suppresses cell proliferation and glucose metabolism via STAT3/SIRT3 signaling pathway in ovarian cancer cells[J]. Cancer Med, 2018, 7(9): 4610-4618.
[20] P-M Ridker, Rane M. Interleukin-6 Signaling and Anti-Interleukin-6 Therapeutics in Cardiovascular Disease[J]. Circ Res, 2021, 128(11): 1728-1746.
[21] M Jia, Li Q, Guo J, et al. Deletion of BACH1 Attenuates Atherosclerosis by Reducing Endothelial

ISSN 2706-6819 Vol.7, Issue 3: 1-16, DOI: 10.25236/IJFM.2025.070301

Inflammation[J]. Circ Res, 2022, 130(7): 1038-1055.
[22] Y Fan, Liu J, Miao J, et al. Anti-inflammatory activity of the Tongmai Yangxin pill in the treatment of coronary heart disease is associated with estrogen receptor and NF-kappaB signaling pathway[J]. J Ethnopharmacol, 2021, 276114106.
[23] R Dorajoo, Ihsan M-O, Liu W, et al. Vascular smooth muscle cells in low SYNTAX scores coronary artery disease exhibit proinflammatory transcripts and proteins correlated with IL1B activation[J]. Atherosclerosis, 2023, 36515-24.
[24] J-J Liu, Jing L-X, Wang J. Correlation of plasma heme oxygenase-1 and matrix metalloproteinase-9 with coronary artery disease[J]. Journal of army medical university, 2018, 40(13): 1247-1250.
[25] N Rani, Arya D-S. Chrysin rescues rat myocardium from ischemia-reperfusion injury via PPAR-gamma/Nrf2 activation[J]. Eur J Pharmacol, 2020, 883173389.
[26] L Ma, Dai X, Wu C, et al. Tanyu Tongzhi Formula Delays Atherosclerotic Plaque Progression by Promoting Alternative Macrophage Activation via PPARgamma and AKT/ERK Signal Pathway in ApoE Knock-Out Mice[J]. Front Pharmacol, 2021, 12734589.
[27] Q Chen, Thompson J, Hu Y, et al. Cardiomyocyte specific deletion of p53 decreases cell injury during ischemia-reperfusion: Role of Mitochondria[J]. Free Radic Biol Med, 2020, 158, 162-170.
[28] Y Cai, Ying F, Liu H, et al. Deletion of Rap1 protects against myocardial ischemia/reperfusion injury through suppressing cell apoptosis via activation of STAT3 signaling[J]. FASEB J, 2020, 34(3): 4482-4496.
[29] R Blanco-Dominguez, de la Fuente H, Rodriguez C, et al. CD69 expression on regulatory T cells protects from immune damage after myocardial infarction[J]. J Clin Invest, 2022, 132(21).
[30] Y-F Song, Zhao L, Wang B-C, et al. The circular RNA TLK1 exacerbates myocardial ischemia/reperfusion injury via targeting miR-214/RIPK1 through TNF signaling pathway[J]. Free Radic Biol Med, 2020, 15569-80.
[31] X Chen, Wang R, Chen W, et al. Decoy receptor-3 regulates inflammation and apoptosis via PI3K/AKT signaling pathway in coronary heart disease[J]. Exp Ther Med, 2019, 17(4): 2614-2622.